Book of Tutorials and Abstracts

European Microbeam Analysis Society

EMAS 2025

18th

EUROPEAN WORKSHOP

on

MODERN DEVELOPMENTS AND APPLICATIONS IN MICROBEAM ANALYSIS

11 to 15 May 2025
at the
TecnoCampus
Mataró (Barcelona), Spain

Organized in collaboration with the
Universitat de Barcelona, Spain

EMAS
European Microbeam Analysis Society eV
www.microbeamanalysis.eu/

This volume is published by:
European Microbeam Analysis Society eV (EMAS)
EMAS Secretariat
c/o Eidgenössische Technische Hochschule, Institut für Geochemie und Petrologie
Clausiusstrasse 25
8092 Zürich
Switzerland

ISBN 978 90 8227 6985
NUR code: 972 – Materials Science

NANOMINERALOGY – PLANETARY MATERIALS

Martin R. Lee

University of Glasgow, School of Geographical and Earth Sciences
Glasgow G12 8QQ, Great Britain
e-mail: martin.lee@glasgow.ac.uk

Martin Lee is a geologist by training, and currently Professor of Planetary Science in the School of Geographical and Earth Sciences, University of Glasgow, UK. The focus of his work is on understanding the earliest history of the solar system including formation of the first mineral grains, and the construction and geological evolution of water-rich asteroids. For this work he studies meteorites and samples returned from asteroids by space missions using techniques including electron backscatter diffraction, transmission Kikuchi diffraction, transmission electron microscopy, and atom probe tomography. Asteroid 8152 Martinlee (1986 VY) is named in his honour.

1. INTRODUCTION

Extraterrestrial materials regularly fall to Earth as gram- to kilogram-size meteorites, and smaller particles of cosmic dust. Meteorites come from the Moon, Mars, asteroids, and possibly also comets, and accordingly can provide a wealth of information on the origin and evolution of the solar system. They can also help us to address the biggest questions in science, including "are we alone?" It is an irony that many of the scientifically most important meteorites, are rare, in particular those from the Moon, Mars and primitive asteroids. Meteorites from the primitive asteroids are also very fragile and hardly ever survive their long journey to Earth, their passage through the atmosphere, and their impact with the ground. It is, therefore, crucial to extract the maximum amount of information from the rarest and most scientifically important meteorite samples whilst destroying the least material.

Meteorites however have their limitations for exploring the solar system. All of them have been contaminated by the terrestrial environment, for example through the addition of water and organic matter – the two compounds that are most important for understanding how and when life could have evolved on other worlds. In addition, we know only very approximately where most meteorites are from (e.g., "the asteroid belt", "Mars"), thus compromising the information that they can provide. The need for pristine samples from known locations has been one of the main drivers of space missions to collect and return samples of extraterrestrial bodies. Most heavily sampled is the Moon, with rocks being returned by six NASA missions (Apollo 11, 12, 14, 15, 16, 17), three Soviet (Luna), and two Chinese (Chang'e 5, 6). NASA has also successfully collected samples from comet 81P/Wild 2 (Stardust mission) and the B-type asteroid Bennu (OSIRIS-REx mission). The Japan Aerospace Exploration Agency (JAXA) has returned fragments of the S-type asteroid Itokawa (Hayabusa mission) and Cb-type asteroid Ryugu (Hayabusa2 mission). These returned samples are extremely precious on account of their uniqueness and scientific importance, the costs of obtaining them and difficulties in obtaining more, and their small size (Table 1). They underscore the value of analysis by minimally destructive nanomineralogical techniques.

Table 1. Samples returned from extraterrestrial bodies.

Target	Mission(s)	Mass returned	Reference
Moon	Apollo	375.9 kg	[3]
Moon	Luna	326 g	[4]
Moon	Chang'e 5	1731 g	[5]
Moon	Chang'e 6	1935 g	[6]
Comet 81P/Wild 2	Stardust	~1 mg	[7]
Asteroid Itokawa	Hayabusa	~0.015 mg	[8]
Asteroid Ryugu	Hayabusa2	5.4 g	[9]
Asteroid Bennu	OSIRIS-REx	121 g	[10]

The final reason why nanomineralogy is so important to planetary science is that the most primitive extraterrestrial bodies (e.g., comets and primitive carbonaceous asteroids) have undergone little or no geological processing since they formed within the protoplanetary disk ~ 4,600 million years ago. These bodies grew by accretion of primordial dust including minerals that originally formed within the atmospheres of stars in another part of the Galaxy. These 'presolar grains' are preserved within meteorites from primitive asteroids [1] and include nanodiamonds with a median size of 2.7 nm (i.e., ~2,000 carbon atoms) [2]. In contrast to comets and carbonaceous asteroids, the larger asteroids, the planets and many of their satellites underwent internal heating leading to metamorphic recrystallisation or melting, and the resulting rocks are typically much coarser grained.

The focus here is on three complementary techniques that are used to obtain nanoscale crystallographic, microstructural, chemical, and isotopic information from extraterrestrial materials: (1) electron backscatter diffraction (EBSD) and transmission Kikuchi diffraction (TKD); (2) transmission electron microscopy (TEM) and scanning transmission electron microscopy (STEM); (3) atom probe tomography (APT). These techniques are always used with prior microscale characterisation by non-invasive or minimally destructive methods including scanning electron microscope (SEM) imaging and energy-dispersive X-ray spectrometry (EDS), electron probe microanalysis (EPMA), and secondary ion mass spectrometry (SIMS).

2. EBSD AND TKD

EBSD has been used extensively to characterise polished samples of asteroidal, martian and lunar meteorites. The most common applications of the technique are to seek evidence for shock metamorphism of these rocks as recorded by the microstructures of mineral grains, and to map crystallographic preferred orientations of polycrystalline samples to explore processes such as low pressure shock, lithostatic compaction, and flow of the rocks when they were molten (e.g., [11-14]).

EBSD is also used to characterise nanoscale properties of planetary materials, and an excellent example is the identification of new minerals (i.e., minerals not previously known to science) in meteorites, and in terrestrial samples, by Chi Ma and colleagues. The new minerals described from meteorites are typically rare and a few micrometres in size. The information needed for them to be classified and named as new minerals has typically come from a combination of EPMA data and the matching of EBSD Kikuchi patterns to the crystal structure of synthetic materials [15]. Techniques including synchrotron X-ray diffraction and Raman spectroscopy have also been combined with EBSD [16]. Between 2009 and 2021 the CV3 carbonaceous chondrite Allende yielded 19 new minerals. Many of them are refractory oxides in calcium- and aluminium-rich inclusions (CAIs), which are among the first solids to have formed after the birth of the solar system [17]. Although Allende and other carbonaceous chondrites have been most

productive, new minerals have also been described from other groups of meteorites including a Ni-silicide in the Norton County aubrite [18], three Fe-phosphates from the El Ali IAB iron meteorite [19], and a high-pressure K-Al silicate from the martian meteorite Zagami [16].

Transmission Kikuchi diffraction (TKD, aka 'transmission electron backscatter diffraction' has been little used to study planetary materials. However, there is now a resurgence of interest in the technique because it can provide high spatial resolution electron diffraction information that is complementary to four-dimensional STEM (4D-STEM, see below). The TKD technique has been comprehensively described by [20] and so is only briefly summarised here. TKD differs from EBSD in that Kikuchi patterns are collected from a thin sample, typically a focussed ion beam (FIB) produced wafer. The electron-beam specimen interaction volume is considerably smaller than for bulk EBSD such that spatial resolutions of a few nanometres can be obtained (depending on the atomic mass of the material being studied) [20]. The deleterious effects of charging are much reduced relative to conventional EBSD, which is advantageous for non-conductive planetary samples. Beam damage can however be a problem for some minerals (e.g., carbonates, phyllosilicates). Elemental data can be collected by EDS simultaneously with the Kikuchi patterns, thus allowing crystallographic data from TKD to be precisely correlated with chemical variations. However, differences in interaction volumes between TKD and EDS may lead to mismatches in precisely locating interfaces and nanograins [20]. As TKD can be undertaken in a suitably equipped FIB microscope, it can be used to characterise the mineralogy of atom probe needles made for APT (see below) without having to transfer them to another instrument [21]. Figure 1 is an example TDK dataset obtained from a particle of asteroid Ryugu. Grains of dolomite and magnetite, < ~1 -2 μm size, are supported in a matrix of nanophase phyllosilicate and Fe-sulphide minerals. Nanostructures within the dolomite grains are twins (Fig. 1c).

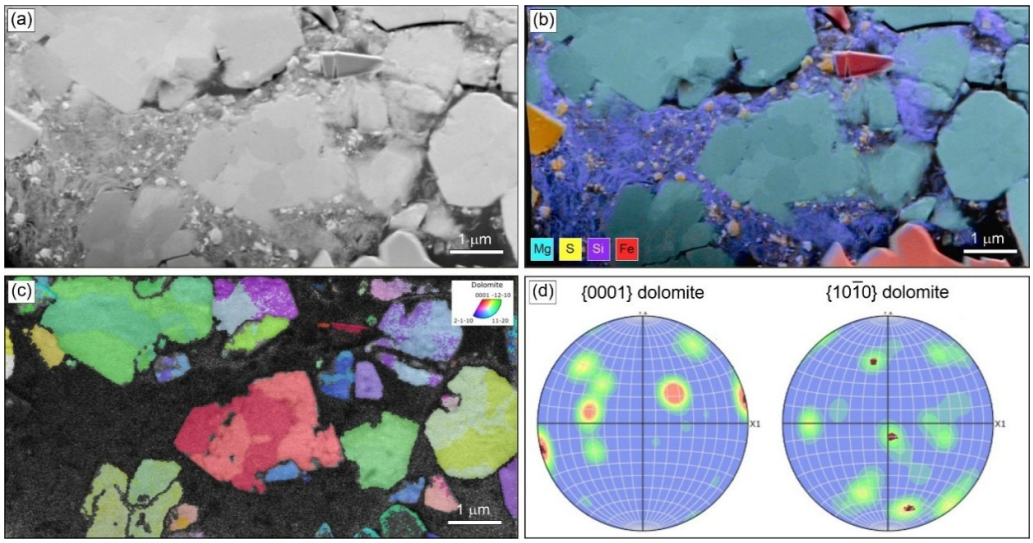

Figure 1. TDK results from dolomite and magnetite in particle A0203 returned from asteroid Ryugu by the JAXA Hayabusa2 mission. a) Forescatter image. b) Multi-element EDS map in which dolomite is cyan, magnetite red, nanophase Fe-sulphide yellow, phyllosilicate blue. c) Dolomite inverse pole figure map. d) Dolomite pole figures. The highlighted points are from the grain in the middle of a) to c).

A pioneering use of TKD to characterise the mineralogy, microstructure and chemical composition of planetary nanominerals was by Daly *et al.* [22]. They studied micrometre to sub-micrometre size metal alloys ('refractory metal nuggets') in several carbonaceous chondrite meteorites. The bulk sample was also characterised by conventional EBSD, and FIB wafers were studied by TEM. The tens of nanometre size constituent grains of refractory metal nuggets were easily resolved, and TDK enabled determination of their mineralogy, their relative crystallographic orientations, the presence and orientation of nanotwins. Likewise, [23] used TKD to characterise grossmanite, perovskite and calcite along with sub-grains and nanotwins within a CAI from the Winchcombe CM carbonaceous chondrite.

TKD also has great potential for quantifying the extent of impact-induced deformation of primitive meteorites and returned asteroid samples from intragranular misorientations within silicate mineral grains. For example, [24] used TDK to describe the nanostructure of olivine in the Allende (CV3) carbonaceous chondrite, which together with conventional EBSD indicated that it had undergone impact-induced compaction. Conversely, TDK showed that olivine grains from asteroid Ryugu have low degrees of misorientation consistent with minimal shock processing [9].

3. TEM AND STEM

TEM and STEM imaging, electron diffraction, EDS, and electron energy loss spectroscopy (EELS) have been used widely for the nanoscale characterisation of planetary materials including asteroidal, lunar and martian meteorites, and samples returned from the Moon, from comet Wild-2, and asteroids Itokawa, Ryugu [9] and Bennu [25]. Within these studies the most commonly used techniques are bright-field, annular dark-field (ADF) and high-resolution imaging, determination of elemental compositions by EDS and EELS, and the identification of minerals and determination of crystallographic orientations by selected area electron diffraction (SAED).

To date, four-dimensional STEM (4D-STEM) [26] has been used little in planetary science yet has enormous potential. Here a convergent electron beam is scanned over the area of interest and an electron diffraction pattern is collected at each point by direct electron detection [27]. The grid of diffraction patterns can then be analysed to explore many different properties of the sample including the minerals present, their crystallographic orientations, intracrystalline nanostructures (e.g., twins) and intracrystalline variations in lattice spacings. The only study of planetary materials to date is Mouloud *et al.* [28], who applied 4D-STEM to samples returned from asteroid Ryugu. They analysed ~1 × 1 μm areas of these very fine-grained polymineralic samples using a 128 × 128 grid. One result that illustrates the power of the technique is with regards to the phyllosilicates. Previous X-ray diffraction and TEM work has shown that Ryugu phyllosilicates include smectite whose crystal structure can expand or contract depending on the amount of interlayer water (d_{001} accordingly ranges from ~ 1.9 to ~ 0.96 nm [28]).

Diffraction patterns showed that smectite is intergrown with Mg-serpentine (lizardite), and smectite d_{001} ranges from ~1 - 2 nm, with a mean of ~1.24 nm (Fig. 2). Such a spacing suggests the presence of interlayer organic matter [28].

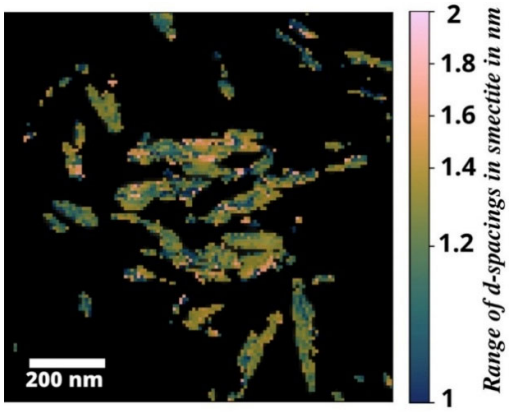

Figure 2. 4D-STEM map of nanoscale variations in the interlayer spacing of smectite crystals in a sample of asteroid Ryugu. Reproduced from Fig. 8b in [28].

4. ATOM PROBE TOMOGRAPHY (APT)

APT is a technique that yields 3D maps of the elemental and isotopic composition of a material at an unrivalled spatial resolution, and as such has huge potential in planetary nanomineralogy. There are several recent comprehensive reviews of the design and operation of APT, and applications in areas including geoscience and planetary science [29-32]. APT can resolve features up to a few tens of nanometres in size with a spatial resolution of ~ 0.3 nm and a sensitivity of ~ 10 atomic part per million (appm). It measures all elements in the periodic table without the need to first select elements of interest nor to calibrate against standards [29]. APT uses needle-shape specimens that are typically < 0.01 μm^3 in volume and ~ 100 nm in apex diameter. For most planetary materials (i.e., non-conductive) the needles are manufactured using a FIB microscope, and although there are several methods one of the most commonly involves cutting and extracting a prism shaped volume from the bulk sample and milling it to a needle (Fig. 3a). Given the size of the needle, the site of interest should be well less than 1,000 nm beneath the sample's surface, and within < 50 nm laterally of the needle's axis [33]. These constraints mean that identifying sites of interest by X-ray mapping can be challenging given the > ~ 200 nm spatial resolution of the technique at ~ 15 - 20 kV [33]. This problem may be circumvented by preparing the needles using a FIB equipped with time-of-flight secondary ion mass spectrometer (ToF-SIMS). Relative to conventional X-ray mapping, ToF-SIMS has a superior lateral resolution (< 50 nm) and detection limits and can measure light elements and isotopes [33]. Once the site of interest has been located (e.g., nanoparticle, sub-grain boundary), a 'button' of platinum can be deposited to serve as a fiducial point to help precisely locate the annular milling [34].

For analysis, atoms and molecular complexes are field evaporated from the tip of a needle under high vacuum and cooled to < 100 K. For conductive specimens, field evaporation is achieved by high voltage, but most planetary materials are also heated via a picosecond laser, usually UV [29]. The single and molecular ions evaporated from the tip are incident on a position-sensitive detector. A time-of-flight mass spectrometer provides information on the mass to charge ratio of the ions and so their identity. The location of the ion's impact on the detector indicates its X-Y position in the needle and the time of its detection its Z-position. The analysed volume of the needle is then reconstructed to make a 3D point cloud of the specimen typically comprising millions of atoms (Fig. 3b).

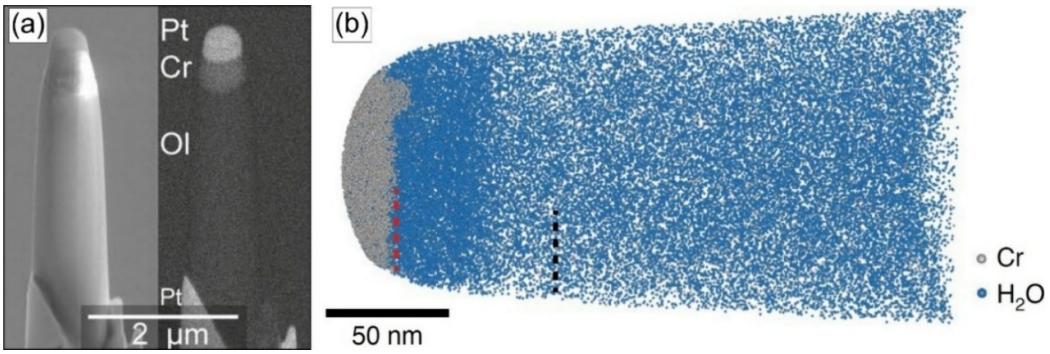

Figure 3. Particle RA_QD02_0279 returned from asteroid Itokawa by the Hayabusa mission. a) Secondary electron (left) and backscattered electron (right) images of a needle that is part-way through annular milling. Layers of FIB-deposited platinum (Pt) and chromium (Cr) have been deposited to protect the olivine (Ol) grain surface. Reproduced from extended data Fig. 1c in [34]. b) APT data showing the 3D distribution of Cr and H_2O ions. The dashed red and black lines delineate the boundaries between the Cr layer and space weathered olivine, and between the space weathered and unweathered olivine, respectively. Reproduced from Fig. 2a. in [34].

As APT yields information on the identity of elements and isotopes and their 3D location it is not a technique for directly characterising crystallinity and crystal structure, or the presence of defects such as dislocations [31]. However, it can be used to detect defects including dislocations and sub-grain boundaries through chemical segregation [29]. An advantage of APT over STEM EDS/EELS is that it can readily measure light elements at low concentrations (H, He, Li), and isotopes. However, various overlaps in the mass-charge spectrum and contamination complicate accurate quantification of the concentrations of certain elements of interest in planetary nanomineralogy. Examples are the overlap between $^{16}O^{+}$ and $^{32}O_2^{2+}$, both with a mass/charge of 16 Daltons [29], and measurement of H being compromised by H in the chamber (this problem may be improved by use of cryo-vacuum transfer systems [32]).

Among the first applications of APT in planetary science were isotopic analysis of nanodiamonds and other presolar grains [35-37], and over the last decade the technique has been applied to meteorites (asteroidal, lunar, martian) and returned samples (lunar and asteroidal) (Table 2).

The most common applications are to determine the elemental compositions of minerals and nanoscale inhomogeneities including element clustering that is an important factor in SIMS-based radiometric dating.

Table 2. Applications of APT in planetary science.

Sample	Target mineral(s)/analyses undertaken	Ref.
Asteroid sample returns		
Asteroid Itokawa	Plagioclase feldspar / Element concentrations	[38]
Asteroid Itokawa	Olivine space weathered rims / Element concentrations & H_2O, OH & H profiles	[34]
Carbonaceous chondrite & iron meteorites		
Winchcombe (CM)	Phyllosilicate / Element concentrations, nanostructure	[39]
Cold Bokkeveld (CM2)	Silicate glass and sulphide nanograins / Element concentrations	[40]
ALH 77307 (CO3.0)	Presolar olivine / Element concentrations & Mg isotope ratios	[41]
QUE 93005 (CM2)	Dolomite & breunnerite / Element concentrations & nanostructures	[42]
Allende (CV3) acid residue	Nanodiamond / Carbon element concentrations & isotope ratios	[2]
Tagish Lake (C2-ung)	Magnetite / Element concentrations & nanostructure	[43]
Tazewell (IAB-sLH iron)	Cloudy zone tetrataenite / Nanostructure	[44]
ALH 77307 (CO3.0)	Refractory metal nuggets / Element concentrations & nanostructure	[45]
North Chile (IIAB) & Bristol (IVA) irons	Kamacite & tetrataenite / Element concentrations & distributions	[46]
Allende (CV3) acid residue	Nanodiamond / Carbon element concentrations & isotope ratios	[47]
Micrometeorites		
Antarctic micrometeorite	Terrestrially weathered micrometeorite / Element concentrations & nanostructure	[48]
Martian meteorites		
NWA 5298	Chlorapatite / Element concentrations & isotope ratios (^{35}Cl, ^{37}Cl).	[49]
NWA 817	Olivine & iddingsite / Element concentrations & nanostructure	[30]
NWA 7034 and pairs	Zircon and baddeleyite / Element concentrations & nanoclusters (Al, Pb)	[50]
Zagami, NWA 6342	Maskelynite and plagioclase feldspar / Element concentrations & nanostructures	[51]
Lunar sample returns and meteorites		
Apollo 17 soil	Olivine & agglutinate / Element concentrations & H, OH, H_2O profiles	[52]
Apollo 17 impact melt breccia	Zircon / Element concentrations & nanoscale distributions (Pb, Y)	[53]
Apollo 17 norite	Apatite / Element concentrations & nanostructure	[54]
Apollo 17 soil	Ilmenite / Element distribution	[55]
Apollo 17 breccia	Zircon / Element nanoclusters & isotope ratios (^{207}Pb, ^{206}Pb)	[56]
NWA 3163 meteorite	Baddeleyite (ZrO_2) / Element concentrations & isotope ratios (^{232}Th, ^{208}Pb)	[57]

Below are three examples of recent applications of APT to planetary materials.

4.1. Identification of extraterrestrial water resources

APT is very effective for locating and quantifying water in planetary materials, and such work is highly relevant to understanding how Earth got its oceans, and the future habitability of the Moon. APT was used by [34] to characterise the outermost ~1 μm of olivine (Mg,Fe_2SiO_4) grains that had been returned from asteroid Itokawa. Results showed that the outermost < 200 nm of grains were enriched in OH and H_2O, which was interpreted to have formed by solar wind derived H^+ combining with the olivine's O (Fig. 3). To verify this mechanism [34] experimentally irradiated terrestrial olivine grains with deuterium (D^+) and using APT showed that the outermost few tens of nanometres of the grains contained D, D_2, DO and D_2O. Such irradiated dust grains could have delivered sufficient water to the early Earth and help make its oceans [34]. APT was also applied to Apollo 17 olivine grains that had been exposed to the solar wind at the lunar surface [52]. Results revealed gradients of decreasing H, OH, and H_2O concentrations from the grain surface to > 100 nm depth.

4.2. Nanoscale mineral intergrowths

Daly *et al.* [42] used APT to characterise nanoscale intergrowths of carbonate minerals within in the CM carbonaceous chondrite Queen Alexandra Range (QUE) 93005. The meteorite is unusual in containing calcite ($CaCO_3$), dolomite ($CaMg(CO_3)_2$), and breunnerite ($(Mg,Fe)CO_3$). The three minerals are intergrown within polymineralic grains and can provide a detailed record of the chemical evolution of the liquid water from which they grew in the interior of an asteroid. Dolomite occurs as a narrow selvage between breunnerite and calcite. Although SEM-EDS showed that it is compositionally homogeneous, APT results demonstrate that it has complex nanostructure comprising ~ 2 nm wide bands of dolomite alternating with breunnerite (Fig. 4). In addition, fluorine- and scandium-rich 'nano-nuggets' are associated with the dolomite bands (Fig. 4). These nanostructures may have formed by crystal growth, or by recrystallisation in response to heating of the asteroid.

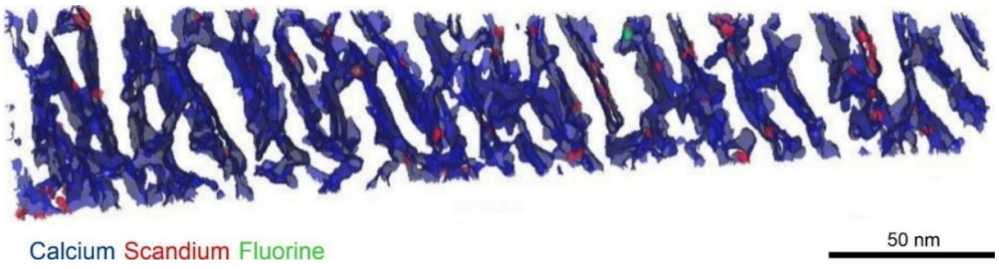

Figure 4. APT reconstruction of a needle extracted from a selvage of dolomite in a polymineralic carbonate grain from QUE 93005. The reconstruction reveals alternating layers of breunnerite (white) with dolomite (blue). Associated with dolomite are 'nano-nuggets' rich in scandium and fluorine. From [42].

4.3. Nanogeochronology of the Moon

Using APT 'nanogeochronology' White *et al.* [57] determined the chronology of crystallisation and shock deformation of a sample of the lunar crust provided by the NWA 3163 meteorite. They analysed baddeleyite (ZrO_2) grains < 10 µm in length. These grains were located by SEM imaging, and their microstructures were initially characterised by EBSD. APT work focussed on baddeleyite grains containing undeformed polysynthetically twinned domains, and containing < 2 µm wide 'patchy domains' that had been produced by later shock. Peaks for ^{208}Pb and ^{232}Th were identified and quantified in the APT mass to charge spectra (Fig. 5). The twinned domain yielded an APT $^{208}Pb/^{232}Th$ age of 4,328 ± 309 million years (Ma), and the patchy domain an APT $^{208}Pb/^{232}Th$ age of 2,175 ± 143 Ma. The same twinned grain was analysed by SIMS and yielded an overlapping $^{207}Pb/^{206}Pb$ age of 4,308 ± 19 Ma. The twinned baddeleyite grain formed at the same time as the host igneous rock and showed that magmatism was ongoing ~ 210 Ma after the Moon formed at 4,150 Ma. The much younger age of the patchy domain correlates with a known episode of impact metamorphism at ~ 2,100 Ma. This study shows that APT can yield accurate radiometric ages and identify lunar events that produce microstructures below the resolution of conventional SIMS-based geochronology (i.e., the patchy domain). However, the APT ages are imprecise owing to the small sizes of the ^{232}Th and ^{208}Pb peaks (Fig. 5). More precise ages would require data from multiple needles manufactured from the same specimen and/or greater APT sensitivity [57].

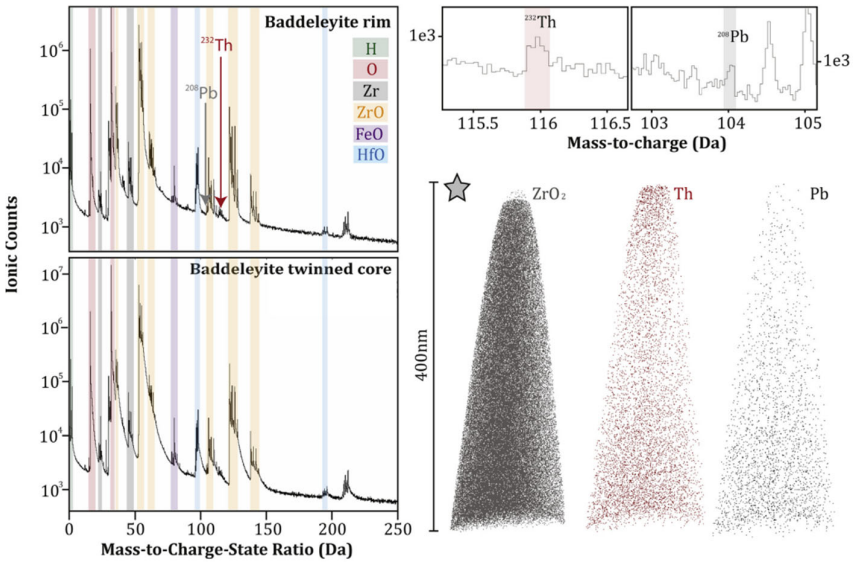

Figure 5. Mass-to-charge spectra, mass-to-charge peaks for $^{232}Th^{2+}$ (116 Daltons) and $^{208}Pb^{2+}$ (104 Daltons), and reconstructions of a needle of baddeleyite from lunar meteorite NWA 3163. Reproduced from Fig. 8 in [57] with permission from Geoscience Frontiers.

5. *SUMMARY AND OUTLOOK*

Nanomineralogical techniques have shown their value for understanding a wide range of extraterrestrial processes including: the composition of the dust from which the solar system formed 4,600 million years ago, documenting geological processes within primitive asteroids, dating key events in the evolution of the Moon and Mars, exploring how Earth got its oceans, and identifying potential reservoirs of water to support future lunar colonies. The coming years promise a revolution in the availability of samples from the Moon, new samples being returned from the moons of Mars, and the return of samples from the surface of Mars that are currently being collected by the NASA Perseverance rover. These samples may be our best chance of finding evidence for extraterrestrial life, and the use of nanomineralogical techniques will be crucial.

6. *ACKNOWLEDGEMENTS*

This work was funded by the UK STFC through grants ST/T002328/1, ST/W001128/1 and ST/T506096/1. For the purpose of open access, the author has applied a Creative Commons Attribution (CC BY) licence to any Author Accepted Manuscript version arising from this submission. The following are acknowledged for the supply of samples, technical help and discussions: Peter Chung, Luke Daly, Cameron Floyd, Wataru Fujiya, Sammy Griffin, Colin How, Laura Jenkins, Pierre-Etienne Martin, Ian MacLaren, Sam McFadzean, William Smith, and Liene Spruzeniece.

7. *REFERENCES*

[1] Lee M R, *et al.* 2025 *Space Sci. Rev.* **221** 11
[2] Lewis J B, *et al.* 2020 *Meteoritics Planet. Sci.* **55** 1382-1403
[3] Jerde A E 2021 *The Apollo programme*. in: *Sample return missions*. (Longobardo A; Ed.) [Amsterdam, The Netherlands: Elsevier] Chapter 2, 9-35
[4] Slyuta E 2021 *The Luna Programme*. in: *Sample return missions*. (Longobardo A; Ed.) [Amsterdam, The Netherlands: Elsevier] Chapter 3, 37-77
[5] Xiao L, *et al.* 2021)*The Chang'e-5 mission*. in: *Sample return missions*. (Longobardo A; Ed.) [Amsterdam, The Netherlands: Elsevier] Chapter 9, 195-206
[6] Cui Z, *et al.* 2024 *Science* **386** 1395-1399
[7] https://curator.jsc.nasa.gov/stardust/samplecollection.cfm
[8] Yoshikawa M, *et al.* 2021) *The Hayabusa mission*. in: *Sample return missions*. (Longobardo A; Ed.) [Amsterdam, The Netherlands: Elsevier] Chapter 6, 123-146
[9] Noguchi T, *et al.* 2024 *Meteoritics Planet. Sci.* **59** 1877-1906
[10] Lauretta D S, Connolly H C Jr., *et al.* 2024 *Meteoritics Planet. Sci.* **59** 2453-2486

[11] Ruzicka A M and Hugo R C 2018 *Geochim. Cosmochim. Acta* **234** 115-147
[12] Cox M A, *et al.* 2022 *Sci. Adv.* **8** eabl7497
[13] Forman L V, *et al.* 2023 *Meteoritics Planet. Sci.* **58** 529-545
[14] Griffin S, *et al.* 2023 *Meteoritics Planet. Sci.* **58** 63-84
[15] Ma C and Rossman G R 2009 *Amer. Mineralogist* **94** 841-844
[16] Ma C, *et al.* 2018 *Meteoritics Planet. Sci.* **53** 50-61
[17] Ma C and Beckett J R 2021 *Meteoritics Planet. Sci.* **56** 96-107
[18] Garvie L A J, *et al.* 2021 *Amer. Mineralogist* **106** 1828-1834
[19] Herd C D K, *et al.* 2024 *Amer. Mineralogist* **109** 2142-2151
[20] Sneddon G C, *et al.* 2016 *Mater. Sci. Eng.: R: Rep.* **110** 1-12
[21] Babinsky K, *et al.* 2014 *Ultramicroscopy* **144** 9-18
[22] Daly L, *et al.* 2017 *Geochim. Cosmochim. Acta* **216** 42-60
[23] Martin P-E, *et al.* 2023 *Chemical and crystallographic characterisation of a grossmanite-bearing calcium-aluminium-rich inclusion within the Winchcombe CM2 carbonaceous chondrite*. in: 54th Lunar Planet. Sci. Conf., abstract #2882
[24] Forman L, *et al.* 2016 *Earth Planet. Sci. Lett.* **452** 133-145
[25] McCoy T J, *et al.* 2025 *Nature* **637** 1072-1077
[26] Ophus C 2019 *Microsc. Microanal.* **25** 563-582
[27] MacLaren I, *et al.* 2020 *APL Mater.* **8** 110901
[28] Mouloud B-E, *et al.* 2024 *Meteoritics Planet. Sci.* **59** 2002-2022
[29] Reddy S M, *et al.* *Geostand. Geoanal. Res.* **44** 5-50
[30] Daly L, *et al.* 2020 *IOP Conf. Ser.: Mater. Sci. Eng.* **891** 012008
[31] Gault B, *et al.* 2021 *Nature Methods Primers* **1** 51
[32] McCarroll I E, *et al.* *MRS Bull.* **47** 696-705
[33] Rickard W D A, *et al.* *Microsc. Microanal.* **26** 750-757
[34] Daly L, *et al.* 2021 *Nature Astronomy* **5** 1275-1285
[35] Heck P R, *et al.* 2010 *Atom-probe tomographic analyses of presolar silicon carbide grains and meteoritic nanodiamonds - First results on silicon carbide*. in: 41st Lunar Planet. Sci. Conf., abstract #2112
[36] Stadermann F J, *et al.* 2010 *Atom-probe tomographic study of the three-dimensional structure of presolar silicon carbide and nanodiamonds at atomic resolution*. in: 41st Lunar Planet. Sci. Conf., abstract #2134
[37] Zinner E K, *et al.* 2011 *Proc. Nat. Acad. Sci. USA* **108** 19135-19141
[38] Jourdan F, *et al.* 2023 *Proc. Nat. Acad. Sci. USA* **120** e2214353120
[39] Daly L, *et al.* 2024 *Meteoritics Planet. Sci.* **59** 1068-1100
[40] Lee M R, *et al.* 2024 *Meteoritics Planet. Sci.* **59** 2818-2830
[41] Nevill N D, *et al.* 2024 *Astrophys. J.* **964** 151
[42] Daly L, *et al.* (2018) *Meteoritics Planet. Sci.* **53** 6239-6239
[43] White L F, *et al.* 2020 *Proc. Nat. Acad. Sci. USA* **117** 11217-11219
[44] Einsle J F, *et al.* 2018 *Proc. Nat. Acad. Sci. USA* **115** E11436-E11445
[45] Daly L, *et al.* 2017 *Geology* **45** 847-850

[46] Rout S S, *et al.* 2017 *Meteoritics Planet. Sci.* **52** 2707-2729
[47] Heck P R, *et al.* 2014 *Meteoritics Planet. Sci.* **49** 453-467
[48] Boyd M R, *et al.* 2023 *Geochim. Cosmochim. Acta* **360** 259-275
[49] Darling J R, *et al.* 2021 *Geochim. Cosmochim. Acta* **293** 422-437
[50] Moser D E, *et al.* 2019 *Nature Geosci.* **12** 522-527
[51] White L F, *et al.* 2018 *Contrib. Mineral. Petrol.* **173** 87
[52] Kling A M, *et al.* 2025 *Earth Planet. Sci. Lett.* **651** 119178
[53] Greer J, *et al.* 2023 *Geochem. Perspectives Lett.* **27** 49-53
[54] Černok A, *et al.* 2021 *Comm. Earth Environ.* **2** 120
[55] Greer J, *et al.* 2020 *Meteoritics Planet. Sci.* **55** 426-440
[56] Blum T B, *et al.* 2019 *Microsc. Microanal.* **25** 2448-2449
[57] White L F, *et al.* 2019 *Geosci. Frontiers* **10** 1840-1848